Effect of available entrainable material on a viscous gravity current

including run-out characteristics and internal flow properties

B. Bates[1] and C. Ancey[1],
[1] École Polytechnique Fédérale de Lausanne,
Laboratory of Environmental Hydraulics

EGU General Assembly, Vienna, Austria, 2013
Session SSP3.2/GM7.15/GMPV46/NH3.16/SSS2.20
Wednesday 10th April, 2013

Outline

1. Numerical simulations
   - The CFD solver
   - Parameter analysis for run-out increase
2. Experimental study
   - The laboratory flume
   - Run-out tracking after entrainment
   - Data acquired using PIV and image processing
   - Internal dynamics in the entrainment zone
3. Concluding remarks

Numerical Simulations

OpenFoam, opensource CFD solver

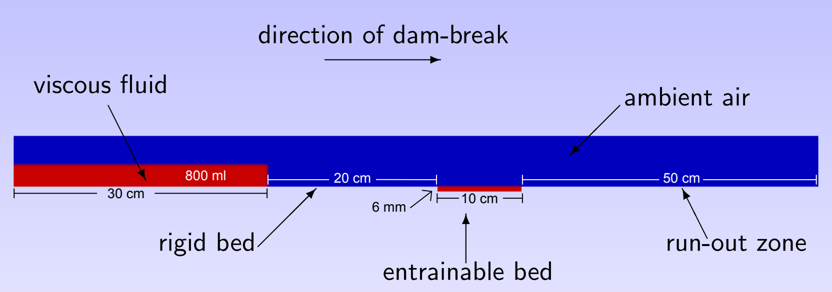

CFD solver: properties

Volume of Fluid phase-fraction solver for two incompressible fluids (interFoam). Viscous fluid is glycerol 98.5%, dynamic viscosity 1.0445 Pa s, laminar flow with Newtonian rheology.

Numerical Simulations

OpenFoam, opensource CFD solver

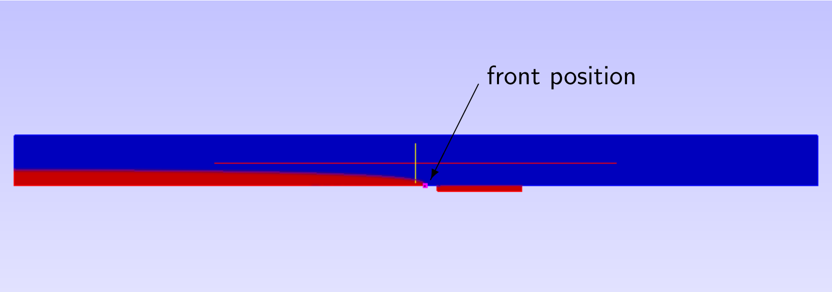

OpenFoam Screenshots

t=2.2 s. Application of contour filter to find front position on rigid bed.

Numerical Simulations

OpenFoam, opensource CFD solver

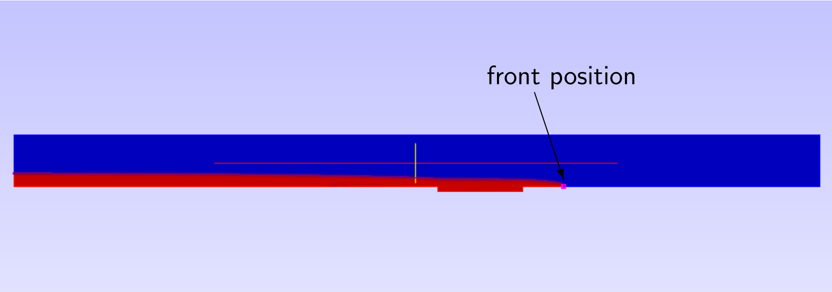

OpenFoam Screenshots

t=7.5 s. Application of contour filter to find front position on rigid bed.

Numerical Simulations

OpenFoam, opensource CFD solver

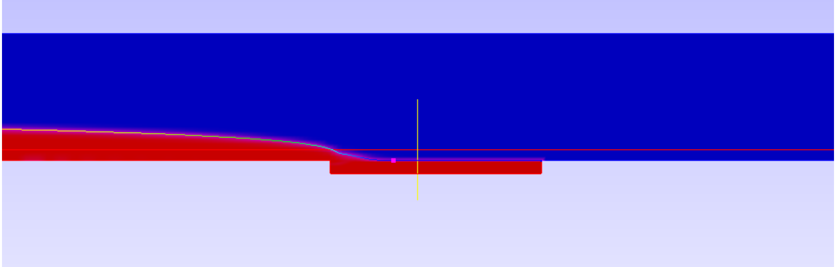

OpenFoam Screenshots

t=2.8 s. Application of elevation filter to find front position on entrainable bed.

Numerical Simulations

OpenFoam, opensource CFD solver

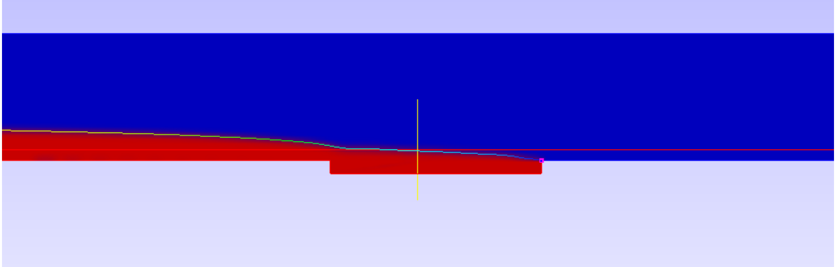

OpenFoam Screenshots

t=4.0 s. Application of elevation filter to find front position on entrainable bed.

Numerical Simulations

Run-out tracking with OpenFoam

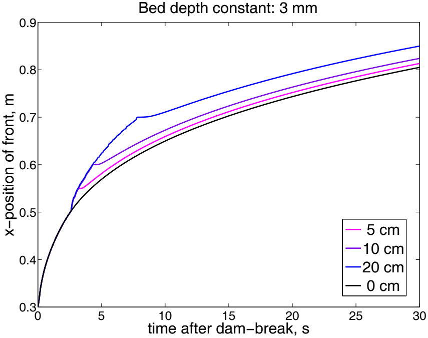

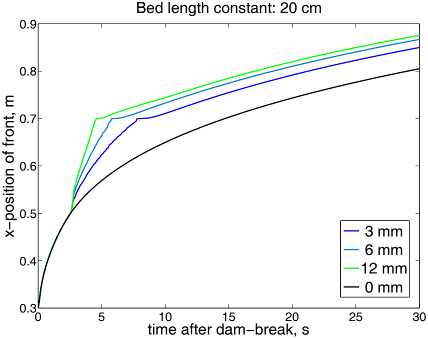

Run-out plots

Plot 1: Bed depth constant: 3 mm, bed length varied: 5 cm, 10 cm, and 20 cm compared with no bed. Plot 2: Bed length constant: 20 cm, bed depth varied: 3 mm, 6 mm, and 12 mm compared with no bed.

Numerical Simulations

Parameter Analysis

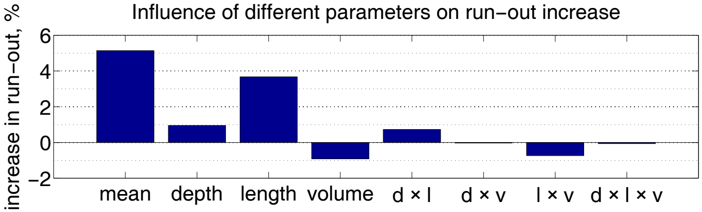

$$Y(\%increase) = 5.14 + 3.67l + 0.96d - 0.92v - 0.73(d \times l) + 0.73(l \times v)$$

Where l is normalized on the interval (5,20) cm, d on the interval (3,12) mm and v on the interval (600,800) ml.

- Increase in front position compared to the no bed case after 30 s (mean =5.14%).
- Bed length was the most important controlling parameter for run-out increase.

Experimental study

The laboratory flume

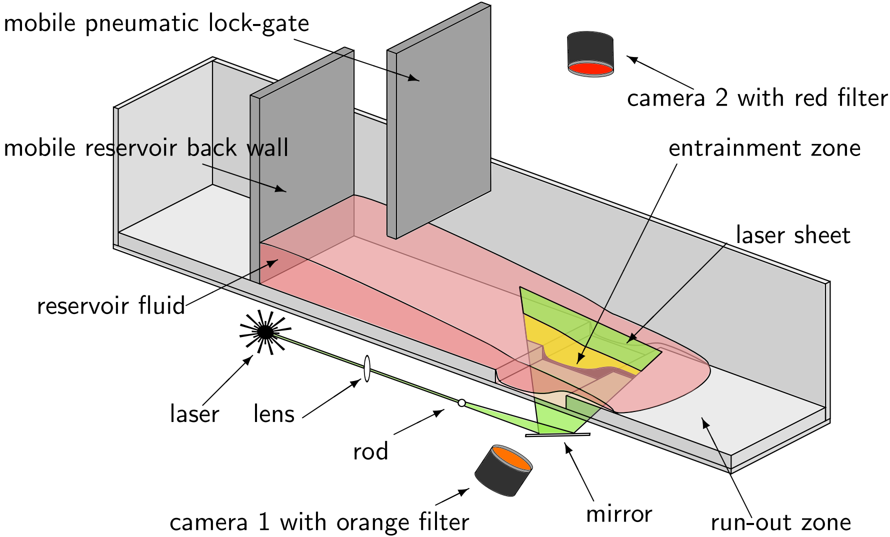

Experimental Study

Cameras: Raw images

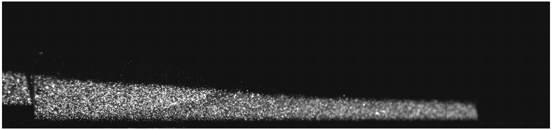

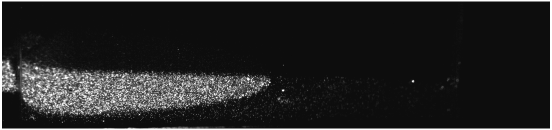

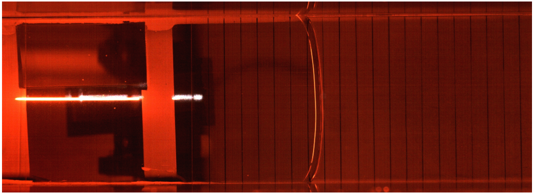

Camera 1

Images of vertical/longitudinal cross-section. Above: 5cm-long by 3mm-deep bed, all dyed for surface identification. Below: 5cm-long by 6mm-deep bed, differentially dyed for interface identification.

Camera 2

Bird's-eye-view of run-out zone, allowing front tracking of run-out.

Bulk Dynamics

Run-out Measurements

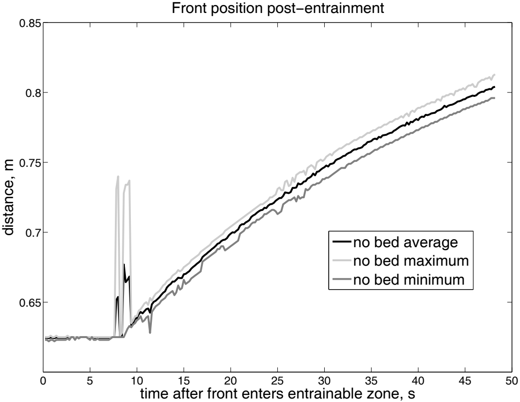

Space-Time plots of flow front

Comparison between the run-out of a no-bed case, a 3 mm-deep bed and a 6-mm deep bed. Bed length is 10 cm.

Bulk Dynamics

Run-out Measurements

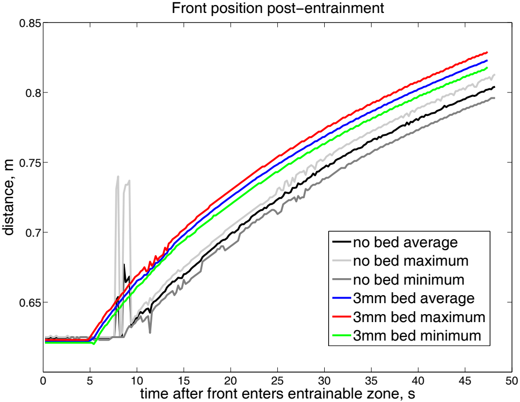

Space-Time plots of flow front

Comparison between the run-out of a no-bed case, a 3 mm-deep bed and a 6-mm deep bed. Bed length is 10 cm.

Bulk Dynamics

Run-out Measurements

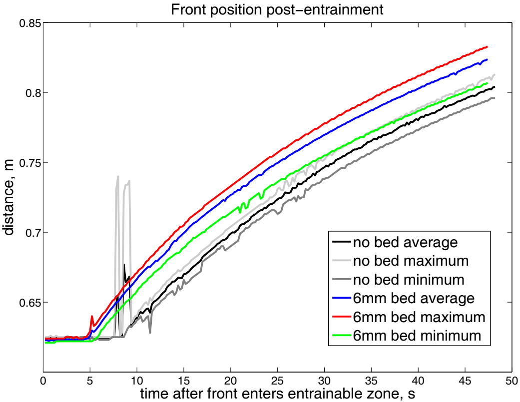

Space-Time plots of flow front

Comparison between the run-out of a no-bed case, a 3 mm-deep bed and a 6-mm deep bed. Bed length is 10 cm.

Bulk Dynamics

Run-out Measurements

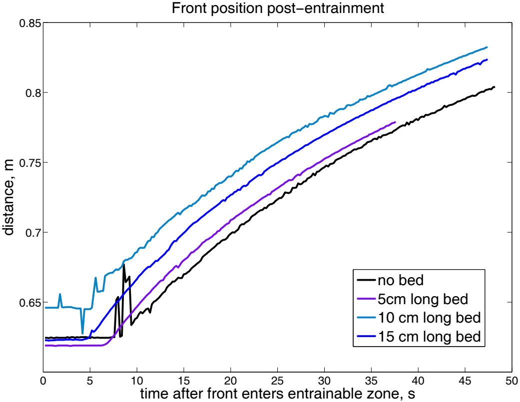

Space-Time plots of flow front

Comparison between the mean run-out of a no-bed case, a 5 cm-long bed, a 10 cm-long and a 15 cm-long bed. Bed depth is 6 mm.

Internal Dynamics

Shear + PIV Profiles

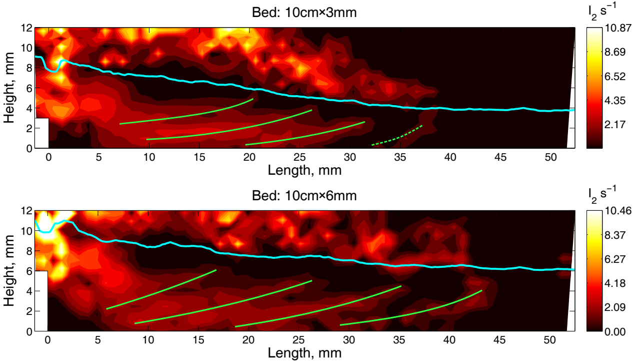

Internal Shear Profiles: All dyed

Second rate of strain invariant: $I_2 = \sqrt{2\left|\frac{\partial u}{\partial x}\frac{\partial v}{\partial y} - \frac{1}{4}\left(\frac{\partial u}{\partial y} + \frac{\partial v}{\partial x}\right)^2\right|}$ s^{-1}, showing regions of high shear. The surface is shown as a reference.

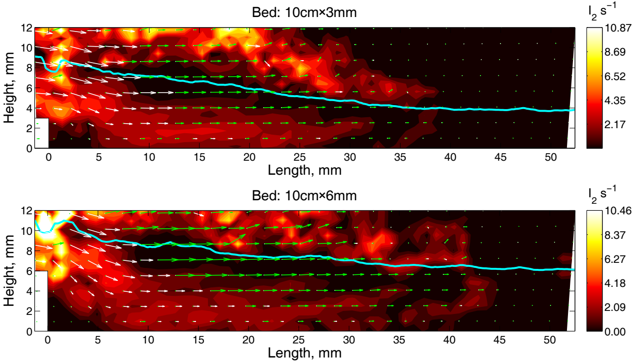

Internal Shear Profiles: All dyed

Second rate of strain invariant: $I_2 = \sqrt{2\left|\frac{\partial u}{\partial x}\frac{\partial v}{\partial y} - \frac{1}{4}\left(\frac{\partial u}{\partial y} + \frac{\partial v}{\partial x}\right)^2\right|}$ s^{-1}, showing regions of high shear. The surface is shown as a reference.

Internal Dynamics

Shear + PIV Profiles

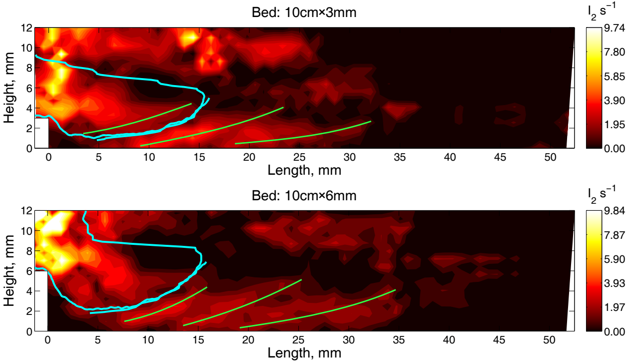

Internal Shear Profiles: Differentially dyed

Second rate of strain invariant: $I_2 = \sqrt{2\left|\frac{\partial u}{\partial x}\frac{\partial v}{\partial y} - \frac{1}{4}\left(\frac{\partial u}{\partial y} + \frac{\partial v}{\partial x}\right)^2\right|}\ s^{-1}$, showing regions of high shear. The interface is shown as a reference.

Internal Dynamics

Shear + PIV Profiles

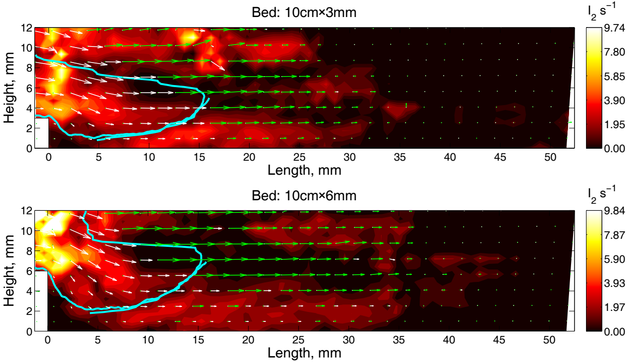

Internal Shear Profiles: Differentially dyed

Second rate of strain invariant: $I_2 = \sqrt{2\left|\frac{\partial u}{\partial x}\frac{\partial v}{\partial y} - \frac{1}{4}\left(\frac{\partial u}{\partial y} + \frac{\partial v}{\partial x}\right)^2\right|}\ s^{-1}$, showing regions of high shear. The interface is shown as a reference.

Internal Dynamics

Shear + PIV Profiles

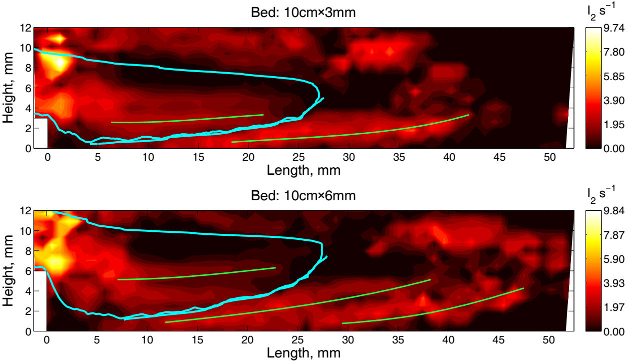

Internal Shear Profiles: Differentially dyed

Second rate of strain invariant: $I_2 = \sqrt{2\left|\frac{\partial u}{\partial x}\frac{\partial v}{\partial y} - \frac{1}{4}\left(\frac{\partial u}{\partial y} + \frac{\partial v}{\partial x}\right)^2\right|}$ s^{-1}, showing regions of high shear. The interface is shown as a reference.

Internal Dynamics

Shear + PIV Profiles

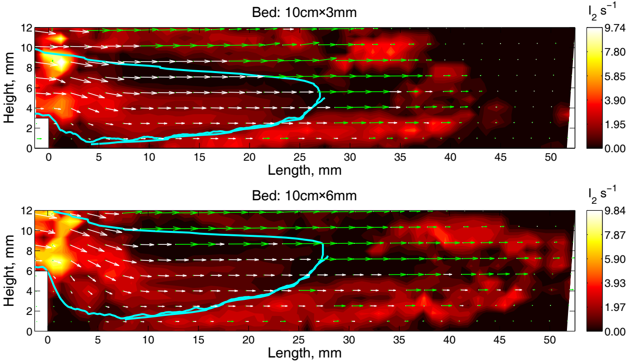

Internal Shear Profiles: Differentially dyed

Second rate of strain invariant: $I_2 = \sqrt{2\left|\frac{\partial u}{\partial x}\frac{\partial v}{\partial y} - \frac{1}{4}\left(\frac{\partial u}{\partial y} + \frac{\partial v}{\partial x}\right)^2\right|}\ \mathrm{s}^{-1}$, showing regions of high shear. The interface is shown as a reference.

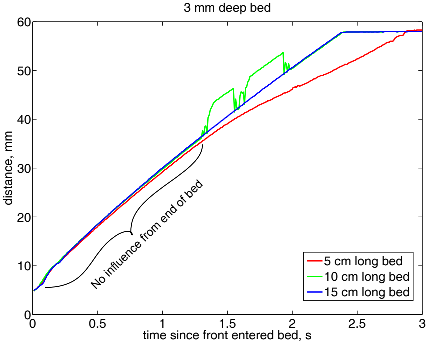

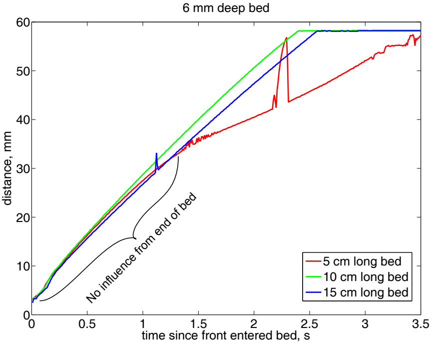

Interface progression plots

Maximum entrainment front position with time. left: Bed depth 3 mm, bed length: 5 cm, 10 cm, and 15 cm. right: Bed depth 6 mm, bed length: 5 cm, 10 cm, and 15 cm.

Conclusion

How does the presence of the bed influence the run-out?

- Numerical and experimental results show entrainment causes an increase in run-out after a finite time.

Conclusion

How does the presence of the bed influence the run-out?

- Numerical and experimental results show entrainment causes an increase in run-out after a finite time.
  - *Parameter analysis: bed length is the most important controlling factor for run-out increase.*

Conclusion

How does the presence of the bed influence the run-out?

- Numerical and experimental results show entrainment causes an increase in run-out after a finite time.
  - *Parameter analysis: bed length is the most important controlling factor for run-out increase.*
- Displaced (entrained) material overflows bed at downstream end, significantly before the entraining front reaches the same position.

Conclusion

How does the presence of the bed influence the run-out?

- Numerical and experimental results show entrainment causes an increase in run-out after a finite time.
  - *Parameter analysis: bed length is the most important controlling factor for run-out increase.*
- Displaced (entrained) material overflows bed at downstream end, significantly before the entraining front reaches the same position.
- Experiments show bed surface uplift and “shear bands”, induced downstream by the entraining front.

Conclusion

How does the presence of the bed influence the run-out?

- Numerical and experimental results show entrainment causes an increase in run-out after a finite time.
  - *Parameter analysis: bed length is the most important controlling factor for run-out increase.*
- Displaced (entrained) material overflows bed at downstream end, significantly before the entraining front reaches the same position.
- Experiments show bed surface uplift and "shear bands", induced downstream by the entraining front.
  - *In a deeper bed, the effects of the incoming front propagate downstream faster.*

Conclusion

How does the presence of the bed influence the run-out?

- Numerical and experimental results show entrainment causes an increase in run-out after a finite time.
    - *Parameter analysis: bed length is the most important controlling factor for run-out increase.*
- Displaced (entrained) material overflows bed at downstream end, significantly before the entraining front reaches the same position.
- Experiments show bed surface uplift and "shear bands", induced downstream by the entraining front.
    - *In a deeper bed, the effects of the incoming front propagate downstream faster.*
- The entraining front slows down after effects of the end of the bed are felt. A longer bed allows the front to travel at a faster speed for longer.

The End

Thank you for your attention

Any questions?

Bibliography

- Andreini, N., Epely-Chauvin, G., Ancey, C. (2012), Internal dynamics of newtonian and viscoplastic fluid avalanches down a sloping bed. *Phys. Fluids*, **24**(5), 053101.
- Bartelt, P., Bühler, Y., Buser, O., Christen, M., Meier, L. (2012), Modeling mass-dependent flow regime transitions to predict the stopping and depositional behavior of snow avalanches. *J. Geophys. Res.* **117**, F01015.
- Eglit, M. E., and Demidov, K. S. (2005), Mathematical modeling of snow entrainment in avalanche motion. *Cold Reg. Sci. Tech.*, **43**(1-2):1023.
- Iverson, R.M., Reid, M.E., Logan, M., LaHusen, R.G., Godt, J.W., Griswold, J.P. (2011), Positive feedback and momentum growth during debris-flow entrainment of wet bed sediment, *Nat. Geosci.* **4**(2), 116–121.
- Mangeney, A., Roche, O., Hungr, O., Mangold, N., Faccanoni, G., Lucas, A. (2010), Erosion and mobility in granular collapse over sloping beds, *J. Geophys. Res.*, **115**, F03040.
- Schürch, P., Densmore, A. L., Rosser, N. J., McArdell, B. W. (2011), Dynamic controls on erosion and deposition on debris-flow fans. *Geol.*, **39**(9):827830.
- Sovilla, B., Burlando, P., Bartelt, P. (2006), Field experiments and numerical modeling of mass entrainment in snow avalanches,*J. Geophys. Res.*, **111**, F03007.

Experimental Study

Runs and Parameters

Table: Camera Properties, Set-up Characteristics, Fluid Properties

Bed Length	5 cm			10 cm			15 cm		
Bed Depth	0 mm	3 mm	6 mm	0 mm	3 mm	6 mm	0 mm	3 mm	6 mm
Volume released	800 ml from reservoir 30 cm long $\times$ 10 cm wide								
Solution Concentration	98.5 % glycerol by weight; 1.5 % distilled water								
Fluid Viscosity	1.0445 Pa s								
Fluid Density	1.2572 g cm^{-3}								
Fluid Temperature	20°C								
	Camera 1 Properties				Camera 2 Properties				
Exposure Time	4.5 ms				10 ms				
Frame Period	8.5 ms				200 ms				
Acquisition Time	10–12 s				40–50 s				